The Journal of Neuroscience, January 15, 1999, *19*(2):813–827

Tenascin-R Inhibits the Growth of Optic Fibers *In Vitro* But Is Rapidly Eliminated during Nerve Regeneration in the Salamander *Pleurodeles waltl*

Catherina G. Becker,[1,2] Thomas Becker,[1,2] Ronald L. Meyer,[2,3] and Melitta Schachner[1,3]

[1]*Zentrum für Molekulare Neurobiologie Hamburg, Universität Hamburg, D-20246 Hamburg, Germany, and* [2]*Department of Developmental and Cell Biology, University of California, Irvine, California 92697*

Tenascin-R is a multidomain molecule of the extracellular matrix in the CNS with neurite outgrowth inhibitory functions. Despite the fact that in amphibians spontaneous axonal regeneration of the optic nerve occurs, we show here that the molecule appears concomitantly with myelination during metamorphosis and is present in the adult optic nerve of the salamander *Pleurodeles waltl* by immunoblots and immunohistochemistry. *In vitro*, adult retinal ganglion cell axons were not able to grow from retinal explants on a tenascin-R substrate or to cross a sharp substrate border of tenascin-R in the presence of laminin, indicating that tenascin-R inhibits regrowth of retinal ganglion cell axons. After an optic nerve crush, immunoreactivity for tenascin-R was reduced to undetectable levels within 8 d. Immunoreactivity for the myelin-associated glycoprotein (MAG) was also diminished by that time. Myelin was removed by phagocytosing cells at 8–14 d after the lesion, as demonstrated by electron microscopy. Tenascin-R immunoreactivity was again detectable at 6 months after the lesion, correlated with remyelination as indicated by MAG immunohistochemistry. Regenerating axons began to repopulate the distal lesioned nerve at 9 d after a crush and grew in close contact with putative astrocytic processes in the periphery of the nerve, close to the pia, as demonstrated by anterograde tracing. Thus, the onset of axonal regrowth over the lesion site was correlated with the removal of inhibitory molecules in the optic nerve, which may be necessary for successful axonal regeneration in the CNS of amphibians.

Key words: CNS injury; optic nerve; retinotectal system; extracellular matrix; amphibians; urodeles

Spontaneous axonal regrowth after a CNS lesion occurs in amphibians and fish but not in mammals (Gaze, 1970; Martin et al., 1994). This difference in regenerative capacity may be attributable to the absence of molecules from the CNS of fish and amphibians that inhibit axonal growth, such as the myelin-associated inhibitor NI35/250 (Caroni and Schwab, 1988; Bastmeyer et al., 1991; Lang et al., 1995; Wanner et al., 1995). However, this issue is controversial (Sivron and Schwartz, 1994; Sivron et al., 1994). Although other molecules with inhibitory activity in mammals, such as the myelin-associated glycoprotein (MAG) (McKerracher et al., 1994; Mukhopadhyay et al., 1994; Schäfer et al., 1996) (but see Bartsch et al., 1995), chondroitin sulfate proteoglycans (CSPGs) (Smith-Thomas et al., 1994; Davies et al., 1997), and tenascin-C (Steindler et al., 1989; Faissner and Steindler, 1995), are present in the CNS of adult amphibians (Becker et al., 1995) and fish (Battisti et al., 1992), the question remains whether these molecules are actually inhibitory for the growth of anamniote axons. An alternative explanation for why regeneration occurs in the CNS of anamniotes is that inhibitory molecules are present but are rapidly removed after an injury. Myelin debris, which contains inhibitors in mammals, is much more rapidly removed from the optic nerve of amphibians than in mammals, similar to the quick removal of debris from the peripheral nervous system of mammals (Perry et al., 1987; Wilson et al., 1992; Sivron and Schwartz, 1995).

We analyzed the expression and function of tenascin-R in the salamander *Pleurodeles waltl.* Tenascin-R is a multidomain and multifunctional extracellular matrix molecule expressed only in the CNS by oligodendrocytes and subpopulations of neurons (Pesheva et al., 1989, 1997; Rathjen et al., 1991; Wintergerst et al., 1993). Tenascin-R is inhibitory for neurite outgrowth from developing mouse cerebellar and chicken retinal explants (Pesheva et al., 1993; Taylor et al., 1993) but not for developing mouse hippocampal neurons, chick dorsal root ganglia, and isolated retinal cells of chicken (Rathjen et al., 1991; Taylor et al., 1993; Lochter et al., 1994, 1995; Lochter and Schachner, 1997). Consistent with an inhibitory function for optic axons, tenascin-R is not present during developmental axonal growth in the optic nerve of mice but is present in the adult (Bartsch et al., 1993). Because inhibition of axonal growth by tenascin-R depends on type and possibly also on developmental stage of neurons (Bates and Meyer, 1997), it is critical to directly demonstrate an inhibitory function for the cell type of interest at a specific developmental stage, in this case retinal ganglion cells of adult *Pleurodeles.*

We show here that tenascin-R immunoreactivity is present in the adult optic nerve of *Pleurodeles* and inhibits optic fiber growth *in vitro*. Elimination of tenascin-R immunoreactivity from the

Received Sept. 2, 1998; revised Nov. 2, 1998; accepted Nov. 4, 1998.

This work was supported by postdoctoral fellowships from the Europen Molecular Biology Organization to C.G.B., the European Union to T.B., and the Deutsche Forschungsgemeinschaft to C.G.B. (Be 1654/2-1) and T.B. (Be 1650/1-1), National Institutes of Health Grant NS26750 to R.L.M., and the Sir Jules Thorn Trust. We thank Drs. Zhi-cheng Xiao and Birgit Hertlein for tenascin-R fragments, Dr. Joanne Taylor for purified tenascin-R, Jill Miotke for introduction to retinal explant culture, Dr. Rita Gerardy-Schahn for the MG5 antibody, and Dr. Udo Bartsch for helpful discussions and critically reading this manuscript.

[3] R.L.M. and M.S. contributed equally to this work.

Correspondence should be addressed to Dr. Catherina G. Becker, Zentrum für Molekulare Neurobiologie Hamburg, Universität Hamburg, D-20246 Hamburg, Germany.

optic nerve at 8 d after crush is associated with the onset of regeneration of optic fibers and may be a necessary condition for successful regeneration within the CNS.

Part of this work has previously been published in abstract form (C. G. Becker et al., 1996; T. Becker et al., 1997a).

MATERIALS AND METHODS

Animals

Larval and adult *Pleurodeles waltl* were taken from our breeding colony. Animals were kept at a 12 hr light/dark cycle. Larvae were fed brine shrimp, and adults were fed beef heart. Developmental stages investigated were early larval (stages 33–34), midlarval (stages 46–48), metamorphic (stages 53–55), and adult (6–8 cm body length). Staging was done according to the method of Gallien and Durocher (1957). Before surgery or killing by transcardial perfusion or decapitation, animals were always deeply anesthetized in 0.1% aminobenzoic acid ethylmethylesther (MS222; Sigma, St. Louis, MO) in PBS, pH 7.2, for 5–15 min, and the depth of anesthesia was tested by tail pinch.

Proteins

In vitro *substrates.* Bovine serum albumin (BSA), tissue culture grade, was purchased from Sigma. Tenascin-R was isolated from adult mouse brains as described previously (Pesheva et al., 1989). The generation of glutathione *S*-transferase (GST) fusion proteins has also been described (Xiao et al., 1996). Here we are using the GST without fusion partner as controls or fused with the epidermal growth factor-like repeats with the cysteine-rich sequences (EGF-L) part of tenascin-R. These fusion proteins were gifts of Dr. Zhi-cheng Xiao from our department.

Antibodies. Monoclonal antibodies 596 and 597 to tenascin-R (Pesheva et al., 1989), and 513 to MAG (Becker et al., 1995) and polyclonal antisera to tenascin-R (Bartsch et al., 1993) and tenascin-C (Becker et al., 1995) have previously been described. Glial fibrillary acidic protein antibody G-A-5 was purchased from Sigma. The neurofilament antibody RT97 and the neurofilament-associated protein antibody 3A10 developed by John Wood (RT97) and Thomas Jessel and Jane Dodd (3A10) were obtained from the Developmental Studies Hybridoma Bank maintained by the University of Iowa (Iowa City, IA) under contract No1-HD-7-3263 from the National Institute of Child Health and Human Development. Antibody MG5 to the neuronal 180 kDa isoform of neural cell adhesion molecule (NCAM) was a gift from Dr. R. Gerardy-Schahn (Medizinische Hochschule Hannover, Hannover, Germany).

Western blot analysis

Cross-reactivity of antibodies 596 and 597 with *Pleurodeles* tenascin-R was determined by Western blot analysis as described earlier (Becker et al., 1995), with the exception that bands of immunoreactivity were visualized using an alkaline phosphatase-coupled secondary antibody with nitro blue tetrazolium and 5-bromo-4-chloro-3-indolyl phosphate as substrates. Some lanes were subsequently washed in 62.5 mM Tris-HCl, 2% SDS, and 100 mM β-mercaptoethanol and immunostained with a polyclonal tenascin-C antibody to exclude cross-reactivity of antibodies 596 and 597 with tenascin-C. Antibody binding was detected with an HRP-coupled anti-rabbit secondary antibody (Dianova, Hamburg, Germany) and visualized with a chemiluminescent substrate (Amersham) according to the supplier's instructions. Blots were exposed on Eastman Kodak (Rochester, NY) X-O-MAT film for 30–90 sec.

Optic nerve lesions

Optic nerve lesions in adult salamanders were performed from a ventral approach as previously described (Becker et al., 1993, 1995). Briefly, holes were drilled into the roof of the mouth of deeply anesthetized salamanders with a dental drill to expose one or both optic nerves just outside the brain case, at a distance of 1.5–1.9 mm from the chiasm. For most experiments the nerve was then crushed with Dumont number 4 forceps. Only for retrograde labeling experiments was the nerve cut with a pair of microscissors (see below). The wound was sealed with dental cement, and the animals were revived in tap water.

Immunohistochemistry

Immunocytochemistry was performed as previously described (Becker et al., 1993, 1995). For immunohistochemical analysis of lesioned optic nerves, only one nerve was crushed, leaving the contralateral nerve as control. Animals were deeply anesthetized and killed by decapitation.

Table 1. Semiquantitative evaluation of anterogradely labeled axons in the lesioned distal optic nerve at different time points after the lesion

Time after crush (d)	Lesion-near half[a]	Chiasm-near half[b]	Chiasm proper[c]
9	−	−	−
9	++	+	−
10	−	−	−
11	+	−	−
11	ND	−	−
11	+	ND	−
11	+++	++	−
13	ND	+++	++
13	ND	+++	++
13	ND	ND	++
15	ND	+++	+++

Each row represents one experimental animal. −, No growth cones; +, more than five growth cones; ++, very numerous growth cones; +++, fasciculated growth, single growth cones obscured; ND, not determined (when nerve segments were lost during staining procedure).

[a]Approximately 0–800 μm distal to the lesion site.

[b]Approximately 800–1600 μm distal to the lesion site.

[c]Entry zone of optic nerve into the diencephalon.

The lesioned nerve and a portion of comparable length of the contralateral unlesioned control nerve were prepared with the brain still attached. Brains and optic nerves were embedded in cryostat mounting medium (Tissue Tek; Sakagura Finetek, Torrance, CA) in such a way that the nerves were bent parallel to the longitudinal axis of the brain. The specimen were quickly frozen, and cross-sections of brain and both optic nerves were cut with a cryostat. Sections of the nerve near the entry point into the chiasm were almost longitudinal (see Fig. 7*L*). Sections were fixed in cold methanol (−20°C) and incubated with the primary antibodies overnight and then with the appropriate fluorescein-labeled secondary antibody (Dianova). Control and lesioned optic nerves were processed on the same microscopic slides. For the developmental study, whole larvae were frozen, cut transversally at the level of the eyes, and processed in the same way as the lesioned nerves. Controls were done by omitting the primary antibody or replacing it with nonimmune mouse or rabbit serum. At least three animals were analyzed for each developmental or postlesion time point.

Anterograde axonal tracing

At varying time points after a unilateral optic nerve crush, animals were reanesthetized, and 2–5 μl of an *N*-hydroxysuccinimidobiotin (Sigma) solution (1.5 mg dissolved in 30 μl of DMSO/30 μl of ethanol) was injected into the vitreal chamber. After 20 hr, salamanders were deeply anesthetized and transcardially perfused with 2% paraformaldehyde and 2% glutaraldehyde in PBS, pH 7.4. Distal parts of lesioned optic nerves were dissected with the brain still attached and cut longitudinally at 50 μm on a vibratome and processed for diaminobenzidine reaction with the ABC kit (Vectastain; Immunodiffusion, Lausanne, Switzerland) as published previously for biocytin tracing (Becker et al., 1997b). Processing the retinas of the injected eye showed intense label within the entire retinal ganglion cell layer, suggesting that most retinal ganglion cells incorporated the tracer. In unlesioned control animals ($n = 3$), strong labeling was observed throughout the optic nerve and diencephalic tract up to the optic tectum. For the semiquantitative analysis of axonal regrowth, the numbers of axons in the lesion-near half (~0–800 μm distal to the lesion site) and the chiasm-near half (~800–1600 μm distal to the lesion site) of the distal lesioned optic nerve as well as the chiasm proper were evaluated as shown in Table 1.

Electron microscopy

Transmission electron microscopy. Unlesioned animals and those that received an optic nerve crush were perfused with 2% paraformaldehyde and 2% glutaraldehyde in PBS. Fifty micrometer vibratome cross-sections of the optic nerve were post-fixed in 1% OsO_4 in 0.01 M phosphate buffer, pH 7.4, for 30 min, washed once in 0.01 M phosphate buffer, dehydrated in an ascending series of acetone, and embedded in

epoxy resin (Spurr's; Plano, Heidelberg, Germany) according to the supplier's specifications. Seventy-five to 100 nm sections were cut on an ultramicrotome (Ultracut S; Leica, Zurich, Switzerland) and collected on Formvar (Merck, Darmstadt, Germany)-coated (0.45% Formvar in chloroform) or uncoated copper grids (M75, Plano). Ultrathin sections were viewed in a JEOL (Tokyo, Japan) 100C electron microscope.

Electron microscopy of anterogradely traced axons. Tracer was applied to one eye, and animals were perfused as described above for anterograde tracing. Fifty micrometer vibratome cross-sections of the optic nerve were reacted to visualize the tracer as described for light microscopy above, with the exception that Triton X-100 was omitted from the procedure (Becker et al., 1997b). Sections were further processed as described for transmission electron microscopy.

Tissue culture

Substrate preparation. All following steps were performed at room temperature, and all dilutions were in PBS, pH 7.2, unless indicated otherwise. Modified 35 mm tissue culture wells with a glass bottom (MatTek, Ashlauch, MA) were coated with nitrocellulose according to the method of Lagenaur and Lemmon (1987). Wells were then coated with poly-[d]-lysine in borate buffer (0.5 mg/ml, pH 8.3) for 8 hr and air-dried. For experiments with a homogeneous substrate, a 25 μl drop of a solution containing 50–100 μg/ml test protein (BSA, GST, EGF-L, or tenascin-R) was spread over the substrate and incubated in a wet chamber overnight. For the demarcation of substrate borders, in a method modified after that of Taylor et al. (1993), a 10 μl drop of sterile filtered india ink (1:100) was coated and immediately aspirated. An 8 μl drop of test protein was pipetted onto the wet india ink spot and incubated overnight. For both substrate preparations, wells were washed with PBS and coated with 2.5 μg of laminin from the basement membrane of Engelbreth-Holm-Swarm mouse sarcoma in 1.5 ml of buffer overnight. Wells were washed with PBS and filled with tissue culture medium.

Efficient coating of tenascin-R was controlled for by antibody staining of cell culture substrates. In experiments with a substrate border, immunofluorescent antibody labeling exactly coincided with the border of the india ink. Coating with nitrocellulose has been shown to yield equal coating efficiency of different tenascin-R fragments elsewhere (Xiao et al., 1996). Coating india ink without test protein did not influence neurite outgrowth. Neutralizing the inhibitory effect of tenascin-R on neurite outgrowth *in vitro* with specific antibodies to tenascin-R in previous experiments has proven difficult because of more than one inhibitory domain being present on the molecule (Taylor et al., 1993; Xiao et al., 1996). In this study, we take the fact that the interactions of axons with the bacterially produced inhibitory EGF-L fragment of tenascin-R (compared with the GST fusion part alone as a control) mimic those with biochemically purified tenascin-R as strong evidence for the specificity of the *in vitro* effects.

Preparation of retinal explants. Animals received a bilateral conditioning optic nerve lesion, either by cutting or by crushing 7 d before retinal explant preparation. The conditioning lesion initiates a regenerative response, which is expressed at the time the explants are made. This allows immediate outgrowth of optic axons, as has been previously shown for fish (McQuarrie and Grafstein, 1981), amphibia (Grant and Tseng, 1986; Taylor et al., 1989), and mammals (Meyer and Miotke, 1990). Animals were deeply anesthetized and decapitated, and the eyes were collected in 70% HBSS. Eyes were quickly rinsed in 70% ethanol, and the retinas were dissected and chopped into 400 × 400 μm squares on a tissue chopper (McIlwain, Gomshall, Great Britain). Squares were washed in HBSS and tissue culture medium consisting of 70% L-15 medium with the following supplements: 20 mM HEPES, 5 μg/ml insulin, 100 μM putrescine, 20 nM progesterone, 100 mg/ml bovine apotransferrin, 30 nM selenium, and 5 μg/ml gentamycin (all purchased from Sigma). Explants were transferred to a medium-filled tissue culture well and oriented with fine forceps to attach to the culture substratum with the vitreous side down. In experiments with a substrate border, explants were placed next to the border. Culture wells were placed in a wet chamber, and neurites were allowed to grow out for 5–7 d.

Immunocytochemistry. After 5–7 d *in vitro*, cultures were washed once in HBSS and twice in 0.1 M phosphate buffer and fixed in 4% paraformaldehyde overnight. They were then washed twice in PBS containing 0.1% Triton X-100 (PBST), incubated in 1.5% goat serum in PBST for 30 min, with primary antibodies in PBST overnight, washed three times in PBST, and incubated with the appropriate FITC- or Cy3-coupled secondary antibodies (Dianova). In controls in which the primary antibody was omitted, only weak nonspecific fluorescence was observed in the explants.

Retrograde labeling of retinal ganglion cells. To specifically label retinal ganglion cells and their processes *in vitro*, a crystal of fluorescein dextran amine (molecular weight, 10,000; Molecular Probes, Eugene, OR) was placed next to freshly cut optic nerves at the time of the conditioning lesion, 7 d before explantation. After 4–7 d *in vitro*, living explants were examined for fluorescence on an inverted microscope using the appropriate filter combinations. Unlabeled explants were used as controls and did not show any fluorescence.

Quantification of substrate interactions. On uniform substrates, all axonal fascicles exceeding 400 μm in length were counted in unfixed cultures on an inverted microscope and given as mean number of neurites per explant. Whether a fascicle was longer than 400 μm was determined with a calibrated objective scale. We considered only long processes for two reasons. Near the explant, fascicles are densely packed, which makes counting more difficult. Moreover, near the explant, short glial processes that resemble neurites could occur under serum-free conditions (Meyer and Miotke, 1990) but are mostly excluded from the analysis by counting long neurites. Because most of the neurites were longer than 400 μm, their number was proportional to the overall outgrowth from a given explant.

For the border experiments, individual interactions of axonal fascicles with the substrate border could not be counted because of the high degree of fasciculation at the border (see Fig. 6*C,D*). Therefore, we scored the number of explants whose axonal fascicles contacted the border but did not cross it, expressing the value as a percentage of all explants analyzed. Explants were still considered inhibited at a border when only very few thin fibers were observed on the substrate side, compared with the thick and numerous fascicles on the explant side that contacted the border. Data were pooled from at least three independent experiments for each test protein and experimental paradigm.

RESULTS

Specificity of tenascin-R antibodies in *Pleurodeles*

Tenascin-R was detected in *Pleurodeles* with two monoclonal antibodies, 596 and 597, raised in mice against chicken tenascin-R, and a polyclonal antiserum against mouse brain tenascin-R (Pesheva et al., 1989). To show that the antibodies are also specific for tenascin-R in *Pleurodeles* and to demonstrate tenascin-R in the CNS of adult *Pleurodeles*, the two monoclonal antibodies, 596 and 597, were used to probe Western blots of retina and brain of adult *Pleurodeles*. Because of limited availability of *Pleurodeles*, it was not possible to isolate enough material from the relatively small optic nerves. Antibodies detected bands of apparent molecular weights at 180 and 160 kDa in the retina (Fig. 1, *lane 1*) and 180 kDa in the brain (Fig. 1, *lane 2*), matching those of mouse tenascin-R (Bartsch et al., 1993). No cross-reactivity with the higher molecular weight bands of the related tenascin-C was detected. The characteristic tenascin-C bands at 190–240 kDa (Becker et al., 1995) were revealed by rehybridizing the nitrocellulose membranes with a polyclonal antiserum to tenascin-C (Fig. 1, *lane 3*). All antibodies to tenascin-R used showed identical staining patterns in immunohistochemistry, which were very similar to those observed in adult mice and chicken (see below) (Rathjen et al., 1991; Bartsch et al., 1993). Specificity was further confirmed by demonstrating the characteristic accumulation of the molecule at nodes of Ranvier (Bartsch et al., 1993) in the spinal white matter of *Pleurodeles* (results not shown).

Immunohistochemical localization of tenascin-R and MAG in the developing and adult retinotectal system

In the mouse optic nerve, tenascin-R is produced by oligodendrocytes (Bartsch et al., 1993). To see whether this is also true for *Pleurodeles*, MAG was always assayed in parallel to tenascin-R immunohistochemistry in the same animals as a marker for the presence of myelinating oligodendrocytes (Becker et al., 1995).

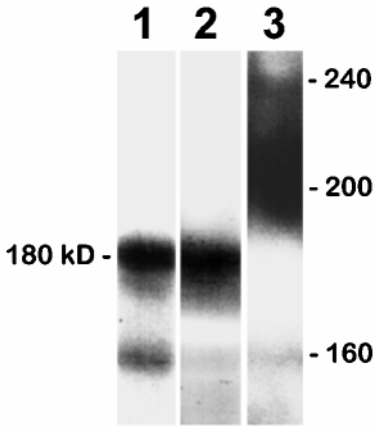

Figure 1. Western blot analysis of tenascin-R (*lanes 1, 2*) and tenascin-C (*lane 3*) in the retina (*lane 1*) and brain (*lanes 2, 3*) of adult *Pleurodeles.* Tenascin-R antibody 597 recognizes a protein band at 180 kDa in the retina and brain and a band at 160 kDa in the retina. Chemiluminescent rehybridization of the same filter depicted as *lane 2* with a tenascin-C antibody, shown as *lane 3*, reveals that there is no cross-reactivity of the tenascin-R antibody with the closely related tenascin-C molecule. The level of the 180 kDa molecular weight marker is indicated on the *left*. Bands of immunoreactivity are indicated on the *right*.

Tenascin-R immunoreactivity could not be detected before metamorphosis in the optic nerve. During metamorphosis (stages 53–55), tenascin-R was expressed in a gradient with strongest labeling near the chiasm (Fig. 2*A,B*). Tenascin-R immunoreactivity was distributed equally throughout the adult optic nerve, except for an area of ~400 μm adjacent to the eye in which it was low (Fig. 2*C*). An accumulation of immunoreactivity at nodes of Ranvier, reported for the optic nerve of mammals (Bartsch et al., 1993), was difficult to determine at the light microscopic level but was readily observed in the spinal white matter, which contains myelinated fibers of larger diameter. Expression of tenascin-R was low in other parts of the pathway of optic fibers during development. In the optic tract, similar to the optic nerve, immunoreactivity for tenascin-R was low during development and high in the adult. In the tectum, tenascin-R was detectable in the deep tectal efferent layers but not in the optic fiber recipient layers from midlarval to adult stages (results not shown). Tenascin-R immunoreactivity appeared in the retina at the time of layer differentiation during early larval development, and this expression remained in the adult retina (Fig. 2*F,G*). Immunolabeling was prominent in the outer plexiform layer and weak in the inner plexiform layer, similar to mice (Bartsch et al., 1993). As in mammals, tenascin-R immunoreactivity was not found in peripheral nerves.

MAG immunoreactivity was not detected in the optic nerve until metamorphosis, when myelin is formed. At metamorphosis, MAG-immunoreactive myelin sheaths formed a gradient in the optic nerve, with myelination being most complete near the chiasm, corresponding to the gradient of tenascin-R immunoreactivity (Becker et al., 1995) (Fig. 2*D,E*). The optic tract was also myelinated during metamorphosis. In adult animals, MAG-immunoreactive myelin sheaths were present throughout the optic nerve and tract, except for the small part in the vicinity of the retina, in which tenascin-R immunoreactivity was also low (Becker et al., 1995). In other parts of the retinotectal system MAG immunoreactivity did not correlate with that of tenascin-R. The retina never becomes myelinated (Becker et al., 1995), and myelination of the tectum was first observed during metamorphosis, using MAG as a marker for myelin (not shown). Thus, myelination of the tectum occurs much later than the appearance of tenascin-R immunoreactivity. Expression of tenascin-R in the retina and the midlarval tectum is likely neuronal. Neuronal expression of tenascin-R has also been found in mice (Fuss et al., 1993; Wintergerst et al., 1993).

Interaction of adult *Pleurodeles* retinal ganglion cell axons with tenascin-R *in vitro*

Because tenascin-R is present in the adult optic nerve, regenerating optic fibers could encounter this molecule *in vivo*. To determine whether tenascin-R might affect the regeneration of optic fibers, retinal explant cultures were made and confronted with the molecule.

Characterization of the retinal explant system

To study interactions of regrowing retinal ganglion cell axons with tenascin-R, a tissue culture system for adult retinal explants was established and characterized. Within 24 hr after explantation, slender, axon-like processes growing out of the explants onto nitrocellulose–poly-[d]-lysine–laminin-coated cell culture substrates were observed. These processes grew to a length of >1 mm within 7 d *in vitro*. Outgrowth of flat, glial cell-like processes was rarely observed. On nitrocellulose–poly-[d]-lysine substrates without laminin no outgrowth was observed ($n = 24$ explants). To show that the processes emanating from these explants were indeed retinal ganglion cell axons, retinal ganglion cells were back-labeled from the optic nerve with fluorescein-dextran-amine at the time of the conditioning lesion *in vivo*. After 4–7 d *in vitro* retinal ganglion cell bodies in the explants and nearly all processes on the culture substrate were clearly labeled (Fig. 3*A,C*). This shows that processes in culture belonged to retinal ganglion cells.

Immunohistochemistry with antibody RT97 to neurofilament proteins confirmed that processes in culture were axons. The antibody was first used *in situ*. It labeled axons of retinal ganglion cells in the retina, but the inner plexiform layer, in which the dendrites of the retinal ganglion cells are located (results not shown), was free of labeling. This indicates that RT97 is a marker for retinal ganglion cell axons, but not dendrites, in *Pleurodeles*. *In vitro*, RT97 prominently labeled fascicles of retinal ganglion cell axons in the explants and processes on the culture substrate emanating from these fascicles (Fig. 3*B,D*), suggesting that processes in culture were axons and not dendrites of retinal ganglion cells.

Immunocytochemical labeling of processes in culture with other neuronal markers, the neurofilament-associated protein antibody 3A10 and the NCAM-180-specific antibody MG5, and the absence of labeling with the GFAP antibody G-A-5, which labeled mostly Müller glia within the explants (results not shown), further supported that processes in culture were neuronal.

Testing retinal ganglion cell axons with a uniform tenascin-R substrate

Retinal explants of adult salamanders were placed on a homogeneous tenascin-R–laminin–poly-[d]-lysine substrate. To control whether an inhibitory effect of the purified whole molecule on retinal ganglion cell axon growth was actually attributable to inhibitory domains of tenascin-R and not to nonspecific interactions or impurities, the inhibitory EGF-L of tenascin-R was tested in the same way. This fusion protein has previously been shown to be inhibitory for neurite outgrowth of embryonic mouse cer-

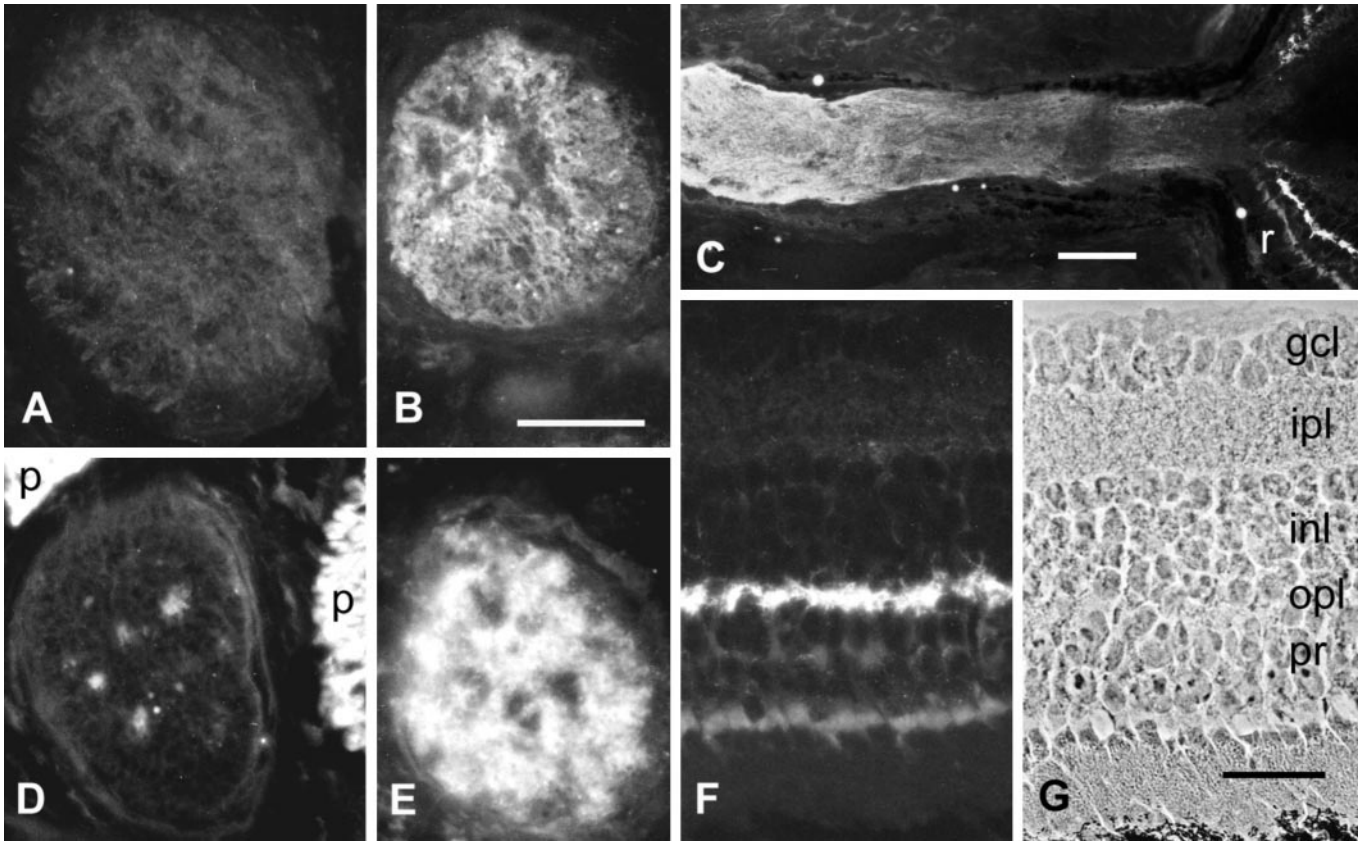

Figure 2. *A–G*, Immunohistochemical localization of tenascin-R (*A–C, F, G*) and MAG (*D, E*) during development. *A–C*, Developmental gradient of tenascin-R expression in the optic nerve. At metamorphosis, tenascin-R immunoreactivity is weak in cross-sections of the optic nerve at the level of the optic foramen (*A*) and strong closer to the chiasm (*B*). *C*, Longitudinal section through the extracranial adult optic nerve with the attached retina (*r*). Tenascin-R immunoreactivity tapers off toward the retina, corresponding to the unmyelinated portion of the optic nerve close to the retina (see Results). *D, E*, MAG immunoreactivity parallels that of tenascin-R at metamorphosis in alternating cross-sections of the of the optic nerve of the same animal shown in *A* and *B* at the level of the optic foramen (*D*, compare with *A*) and closer to the chiasm (*E*, compare with *B*). Peripheral nerves (*p*) in *D* are also strongly labeled with the MAG antibody. *F, G*, Immunofluorescent (*F*) and phase-contrast (*G*) images of a cross-section through the adult retina. Labeling with tenascin-R antibodies is prominent in the outer plexiform layer. Fluorescence of the inner segments of the photoreceptors is nonspecific. *gcl*, Ganglion cell layer; *ipl*, inner plexiform layer; *inl*, inner nuclear layer; *opl*, outer plexiform layer; *pr*, layer of photoreceptor somata. Scale bars: *B*, 50 μm (for *A, B, D, E*); *C*, 100 μm; *G*, 50 μm (for *F, G*).

ebellar explants (Xiao et al., 1996). Outgrowth on tenascin-R and EGF-L was compared with BSA and GST without a fusion partner as control proteins. On control substrates outgrowth of numerous long neurites was indistinguishable from the growth observed on laminin alone (Fig. 4*A,B*). On tenascin-R- or EGF-L-containing substrates the number of processes that grew out of the explants was drastically reduced (Fig. 4*C,D*). Outgrowth of flat, glia-like processes was rarely observed on any substrate.

To quantify the effect of different substrates, the total number of axonal fascicles that were ≥400 μm in length was determined for different substrates and is given here as mean number of fascicles per explant (see Materials and Methods). These values are 12.81 ± 2.9 (SEM) on BSA (n = 11 explants) and 8.97 ± 1.18 on GST (n = 38 explants). These numbers were at least nine times higher than those observed on tenascin-R (0.13 ± 0.076; n = 32 explants) and EGF-L (1.14 ± 0.22; n = 59 explants) (Fig. 5*A*). The differences between controls and tenascin-R or EGF-L were highly significant (ANOVA on ranks, $p < 0.001$). The two controls, BSA and GST, were not significantly different from each other (p = 0.258). Thus, tenascin-R inhibited outgrowth of retinal ganglion cell axons onto the culture substrate, most likely because of interactions with inhibitory domains of the molecule.

Testing retinal ganglion cell axons with a substrate border

To distinguish between the possibilities that tenascin-R inhibits axonal growth directly or merely prevents the axons from growing out of the explants, fibers were allowed to exit the explants and to grow into a sharp border of test protein in the presence of laminin. When reaching the border, neurites did not cross it to grow into regions that contained tenascin-R or EGF-L. Axons were often observed to make sharp turns at the border and to grow along the circumference of the substrate spot with the growth cone making filopodial contact with the test substrate (results not shown).

It was not possible to quantify the border interaction by counting individual crossing events because of strong fasciculation at the border. Therefore, we counted the number of explants whose axons did not cross the border and give these as a percentage of the total number of explants analyzed for the different substrates (see Materials and Methods). Only 7% of the explants showed inhibition of their axons at a BSA border (n = 14 explants), and no inhibition was observed at GST borders (n = 31 explants). In contrast, retinal ganglion cell axons from 60% of the explants were inhibited at a tenascin-R border (n = 35 explants), and 87%

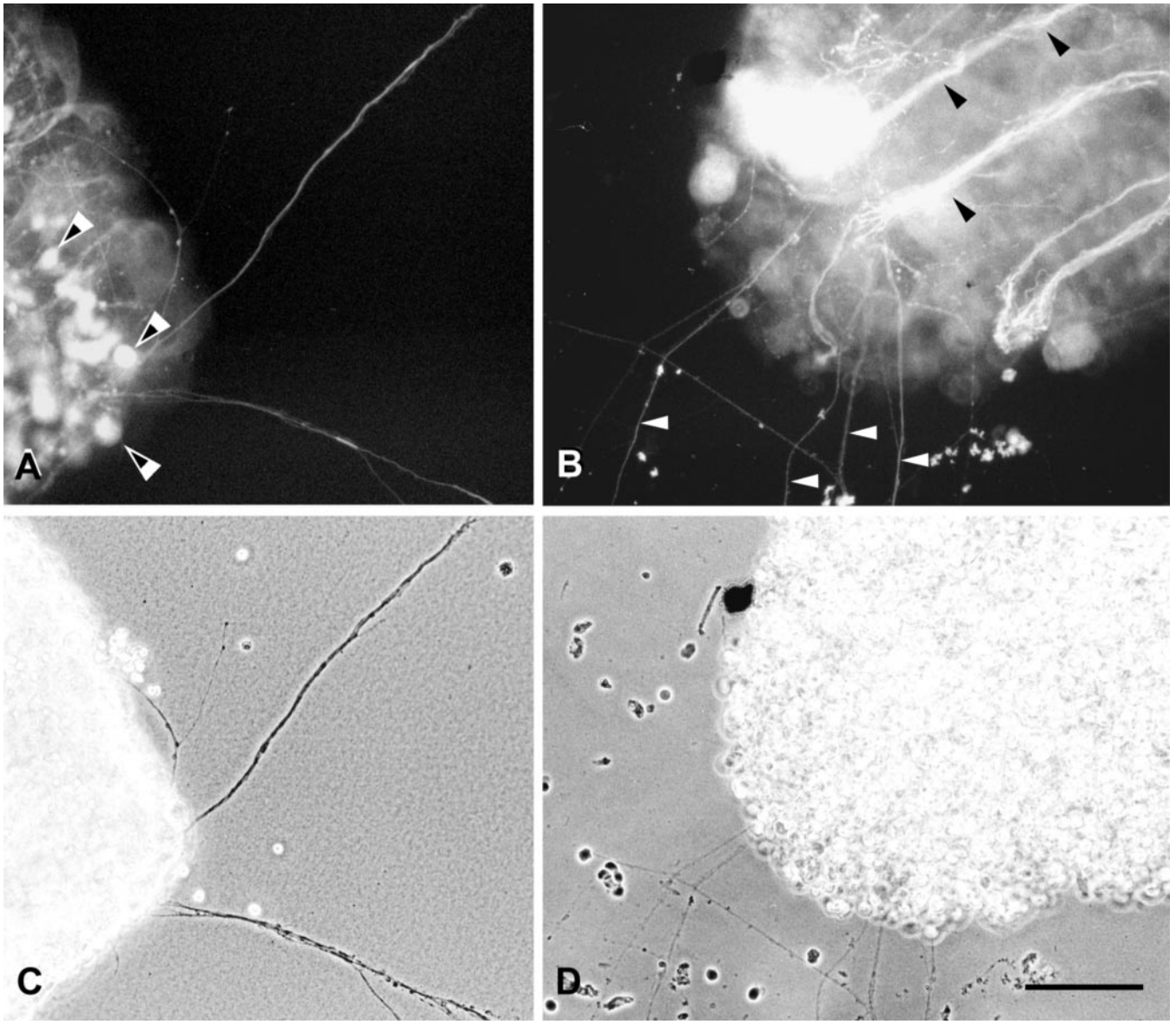

Figure 3. *A–D*, Identification of cellular processes in retinal explant culture. *A*, Previous retrograde labeling with fluorescein-dextran-amine *in vivo* labels retinal ganglion cell somata within the explant (*arrowheads*) and nearly all processes on the cell culture substrate. Compare with phase-contrast image (*C*). *B*, RT97 immunocytochemistry labels fascicles of retinal ganglion cell axons within the explant (*black arrowheads*) and processes on the cell culture substrate (*white arrowheads*). *D*, Phase-contrast image of the explant depicted in *B*. Processes in explant culture are most likely retinal ganglion cell axons. Scale bar, 100 μm.

were inhibited at an EGF-L border ($n = 31$ explants) (Figs. 5*B*, Fig. 6*A–D*). Pair-wise comparisons of different treatments using Fisher's exact test showed significant ($p < 0.001$) differences between test proteins (tenascin-R and EGF-L) and controls (BSA and GST). Retinal ganglion cell axons were mostly prevented from growing from a laminin substrate onto a mixed tenascin-R–laminin or EGF-L–laminin substrate. Thus, in both *in vitro* assays, retinal ganglion cells did not extend axons onto tenascin-R or EGF-L substrates.

Postinjury changes in tenascin-R and MAG immunoreactivity

The preceding studies showed that tenascin-R is present in the adult optic nerve of *Pleurodeles*. Because optic nerves do regenerate *in vivo*, immunohistochemistry was used to find out whether tenascin-R remains in the optic nerve after a crush. MAG immunohistochemistry was also performed to monitor myelin breakdown and remyelination of the lesioned optic nerve.

Tenascin-R immunoreactivity was rapidly lost from the distal optic nerve after the lesion. After 4–6 d it was strongly reduced in the distal lesioned optic nerve (results not shown). At 8 d after the lesion (Fig. 7*A–C*) immunolabeling was reduced to undetectable levels throughout the distal lesioned optic nerve (compare Fig. 7*D*). Tenascin-R immunoreactivity reappeared in the distal optic nerve between 3 and 6 months after the lesion (Fig. 7*H,I*). Note that at 6 months after the lesion, MAG immunoreactivity was confined to myelin sheaths (Fig. 7*K*), whereas tenascin-R immunoreactivity appeared evenly distributed throughout the nerve cross-section, probably reflecting extracellular deposition of the molecule on a variety of different cellular structures (Fig. 7*I*). This apparently uniform deposition of tenascin-R may be

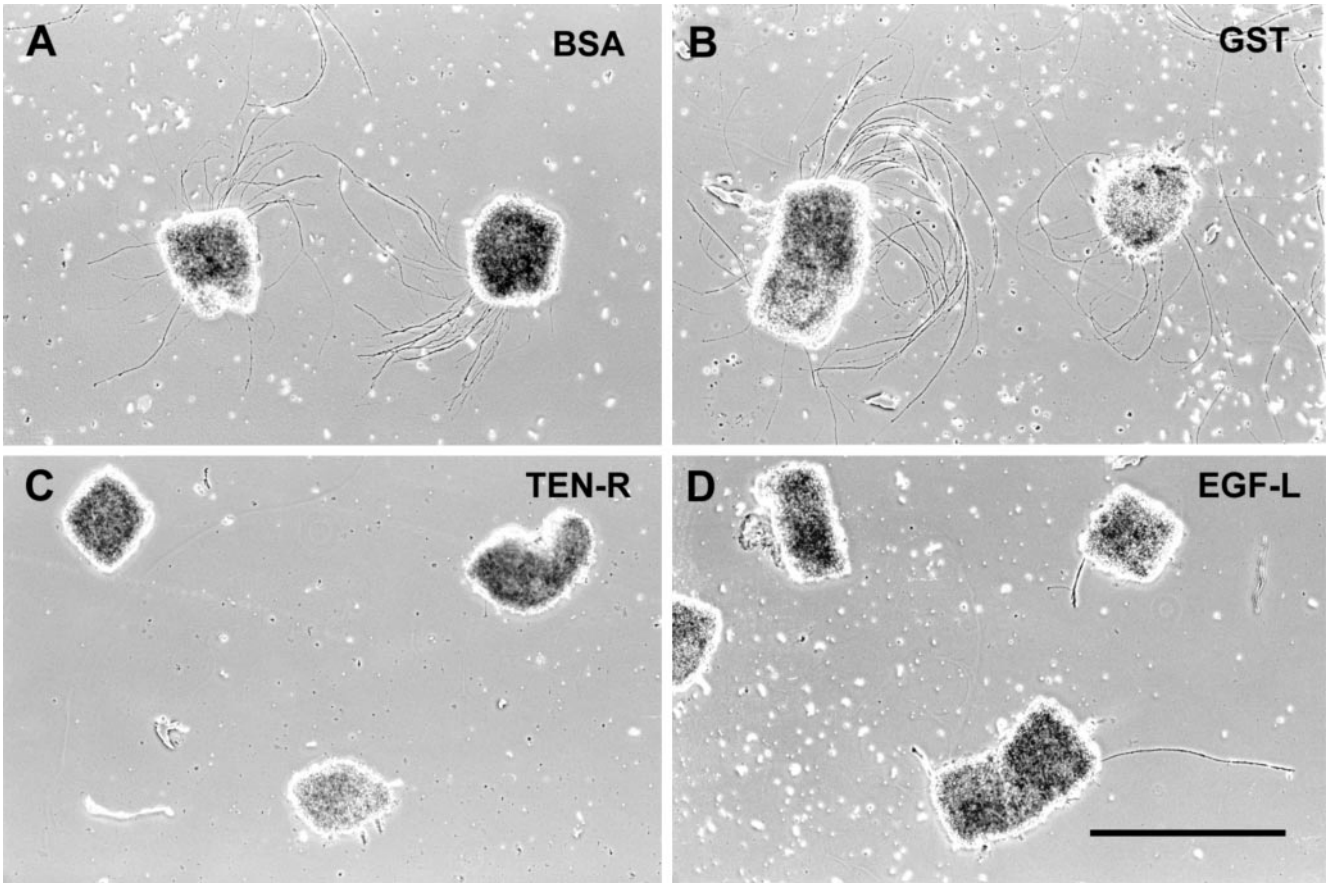

Figure 4. Outgrowth of retinal ganglion cell axons from retinal explants on homogeneously coated substrates at 7 d *in vitro*. *A, B*, On control substrates, with either BSA–laminin (*A*) or GST–laminin (*B*) robust outgrowth occurs. *C*, On a tenascin-R–laminin substrate no outgrowth was observed. *D*, On an EGF-L–laminin substrate outgrowth is very scarce. Scale bar, 1 mm.

attributable to an overproduction by the remyelinating oligodendrocytes, so that myelinated fibers were no longer the preferred tenascin-R-immunoreactive structures. In the optic tract, similar to the distal lesioned optic nerve, tenascin-R immunoreactivity was lost during regeneration. No changes of the normal adult pattern of immunoreactivity (see above) were observed in the proximal optic nerve stump and the tectum after optic nerve crush.

After a crush, MAG immunoreactivity was also rapidly lost from the distal optic nerve. At 6 d after the lesion MAG-immunoreactive myelin debris was observed throughout the lesioned distal nerve, but in contrast to the myelin patterns observed in unlesioned control or remyelinated nerves (Fig. 7*E,K,L*), the immunoreactivity appeared scattered, indicating degenerating myelin (compare Fig. 7*G*). At 8 d after the lesion, the lesion-near half of the optic nerve was free of MAG immunoreactivity (Fig. 7*F*), but in the chiasm-near half, MAG immunoreactive myelin debris remained in a small area close to the chiasm for at least 14 d after the lesion (Fig. 7*G*). The pattern of MAG immunoreactivity was very similar to the distribution of myelin found by electron microscopy during the same period (see below), indicating that MAG immunoreactivity is a valid marker for myelin in *Pleurodeles.* At 3 months after the lesion a few individual MAG immunoreactive myelin sheaths could again be detected with highest density near the chiasm in two of three animals (Fig. 7*J,L*). In one animal only myelin debris was present at the chiasm, similar to what was observed at 14 d after the lesion. The number of MAG-immunoreactive sheaths was increased and equally distributed throughout the nerve at 6 months after the lesion, but labeled myelin sheaths were fewer than in unlesioned control nerves (Fig. 7*K*). Unequal distribution of myelin sheaths along the longitudinal axis of the optic nerve at 3 months but not 6 months after the lesion suggests that remyelination starts at the chiasm and may be complete by 6 months after the lesion. Thus, clearance of tenascin-R immunoreactivity occurring within 8 d after the lesion in the distal optic nerve is even faster than that of MAG (Fig. 7, compare *C,G*). However, most MAG-immunoreactive debris may be phagocytosed (see below), such that the time course of MAG removal from the extracellular environment in the optic nerve may be similar to that of tenascin-R. Reappearance of tenascin-R immunoreactivity between 3 and 6 months after the lesion coincides with remyelination of the optic nerve, which was determined by the reappearance of MAG immunoreactivity.

Time course of regrowth of retinal ganglion cell axons

To find out how closely axonal regrowth into the lesioned distal optic nerve correlates with the reduction of tenascin-R immunoreactivity, regenerating axons were labeled by tracer injections into the eye. Growth of axons was analyzed in cross-sections or longitudinal sections of the distal optic nerve and the chiasm (Fig. 8). At 9–11 d after the lesion incipient fiber growth was observed close to the lesion site in the distal optic nerve stump (Fig. 8*A,C*). Protrusions at the tip of the labeled axons were identified as

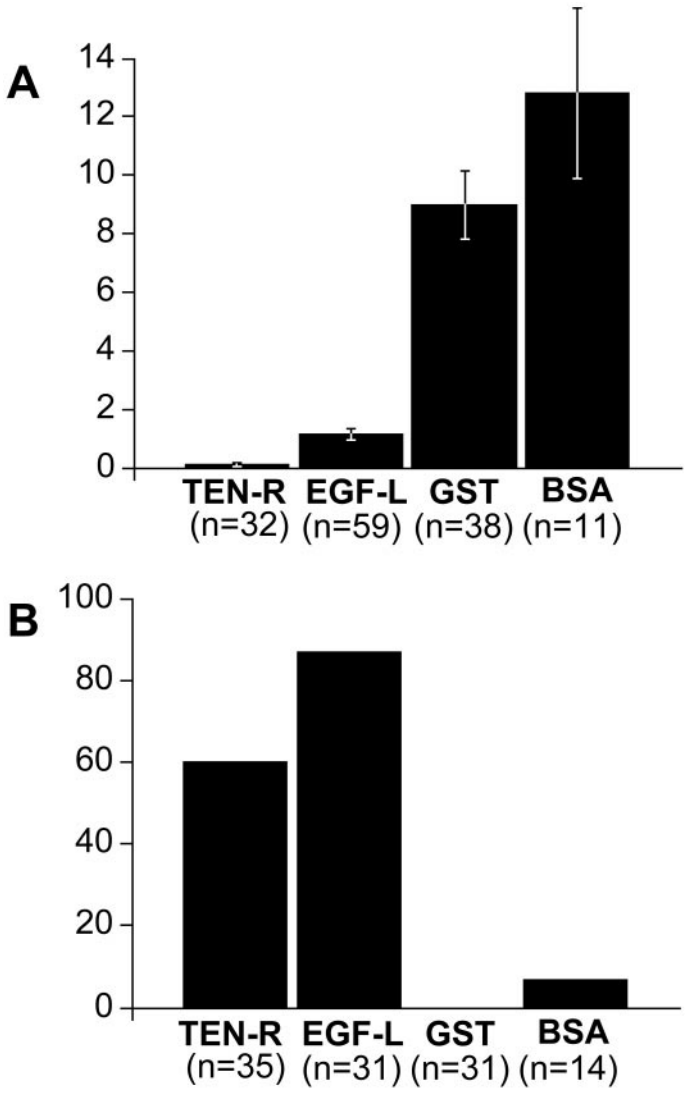

Figure 5. Quantification of axonal growth of retinal ganglion cells *in vitro* on a homogeneous substrate (*A*) or in a border situation (*B*). *A*, Values give the average number of neurites per explant ± SEM. Outgrowth on tenascin-R and EGF-L substrates is highly significantly (ANOVA on ranks, $p < 0.001$) reduced, compared with controls (GST, BSA). *B*, Values indicate the percentage of explants whose axons were strongly inhibited at a substrate border. Inhibition at a tenascin-R and EGF-L border is significantly (Fisher's exact test, $p < 0.001$) higher than in controls (GST, BSA). *TEN-R*, Tenascin-R; *n*, number of explants per treatment.

growth cones (Fig. 8*C*). The first axons reached the chiasm at 13 d after the lesion (Fig. 8*B,D*). At 15 d after the lesion large numbers of axons showed fasciculated growth into the chiasm. Individual growth cones were observed in the diencephalic optic tract close to the pial surface (results not shown).

For a semiquantitative analysis of axonal regrowth, the nerve was divided into three parts, a lesion-near half, a chiasm-near half, and the chiasm proper. Regrowth in each of these compartments was evaluated according to the criteria given in Table 1. Although some variability in the speed of axonal regrowth between different animals was observed, a clear progression of growth through the distal nerve segment could be determined between 9 and 15 d after the lesion (Table 1). We conclude that regrowth into the distal optic nerve starts at ~9 d after the optic nerve crush, when tenascin-R immunoreactivity is lost.

Cellular substrates of regenerating axons

To find out the cellular substrates that regenerating axons were using during regeneration, the environment of regenerating axons was investigated using electron microscopy.

Myelin sheaths found in unlesioned nerves (Fig. 9, *inset*) were completely removed at 9 d after the lesion between the lesion site and ~800 μm distal to it but remained in the chiasm near-part of the nerve, confirming results from MAG immunohistochemistry. In this area, the circumferential zone of the optic nerve near the pia, through which most regenerating axons will grow, was likewise free of myelin (results not shown). At 14 d after the lesion, myelin debris was still present in a small area in the vicinity of the chiasm at a distance of up to 300 μm from the chiasm toward the eye. Myelin debris was phagocytosed by cells with an electron-dense cytoplasm. These cells were preferentially associated with the pial surface at 14 d after the lesion (Fig. 9). Occasionally, these cells could also be observed outside the nerve proper (results not shown). They may therefore be macrophages that had invaded the nerve and left it again through the pial surface.

To determine which cellular components the axons were contacting, the first regenerating axons were anterogradely labeled by tracer injections into the eye in the same way as for the light microscopic analysis. Cross-sections of the distal lesioned optic nerve were analyzed at 9 d after the lesion. Axons regrew in fascicles in the periphery of the nerve (Fig. 10*A*) with the number of axons belonging to a fascicle decreasing with the distance from the lesion site (Fig. 10*B,C*). In the peripheral zone, which was free of myelin debris throughout the entire length of the optic nerve, pioneering single axons and small bundles of labeled axons were found mostly in close contact with the inner surface of large unlabeled protrusions abutting the pial surface. These processes end in a thick and relatively straight centripetal process and were tentatively identified as endfeet of radial astrocytes (Fig. 10*A*). These endfeet formed processes that appeared to be actively enwrapping these newly growing fascicles (Fig. 10*B*). In the area of the nerve closest to the chiasm in which myelin remained for longer times (see above), only one labeled axon was observed contacting myelin debris. Thicker fascicles in the vicinity of the lesion site were tightly enwrapped by glial processes (Fig. 10*C*). Similar observations have been made by transmission electron microscopy in the newt *Triturus viridescens* (Stensaas and Feringa, 1977) and by immunohistochemistry for axonal markers at the light microscopic level in *Pleurodeles* (Becker et al., 1993). Thus, axons regrew in fascicles and were mostly associated with glial processes in the periphery of the nerve.

DISCUSSION

We show here that tenascin-R is present in the adult optic nerve of *Pleurodeles* and that it is strongly inhibitory for adult retinal ganglion cell axons *in vitro*. When the optic nerve is crushed tenascin-R immunoreactivity is lost at the time that axons regrow. Removal of tenascin-R and other molecules may be important for permitting axonal regeneration.

Tenascin-R is present in the CNS of salamanders

Tenascin-R in the adult CNS of *Pleurodeles* was detected using cross-reactive antibodies in immunoblots and immunohistochemistry. So far the molecule has been demonstrated in mammals (Pesheva et al., 1989) and birds (Rathjen et al., 1991) but not in anamniotes. The fact that bands of identical apparent molecular weight as those in mice (Bartsch et al., 1993) at 160 and 180 kDa

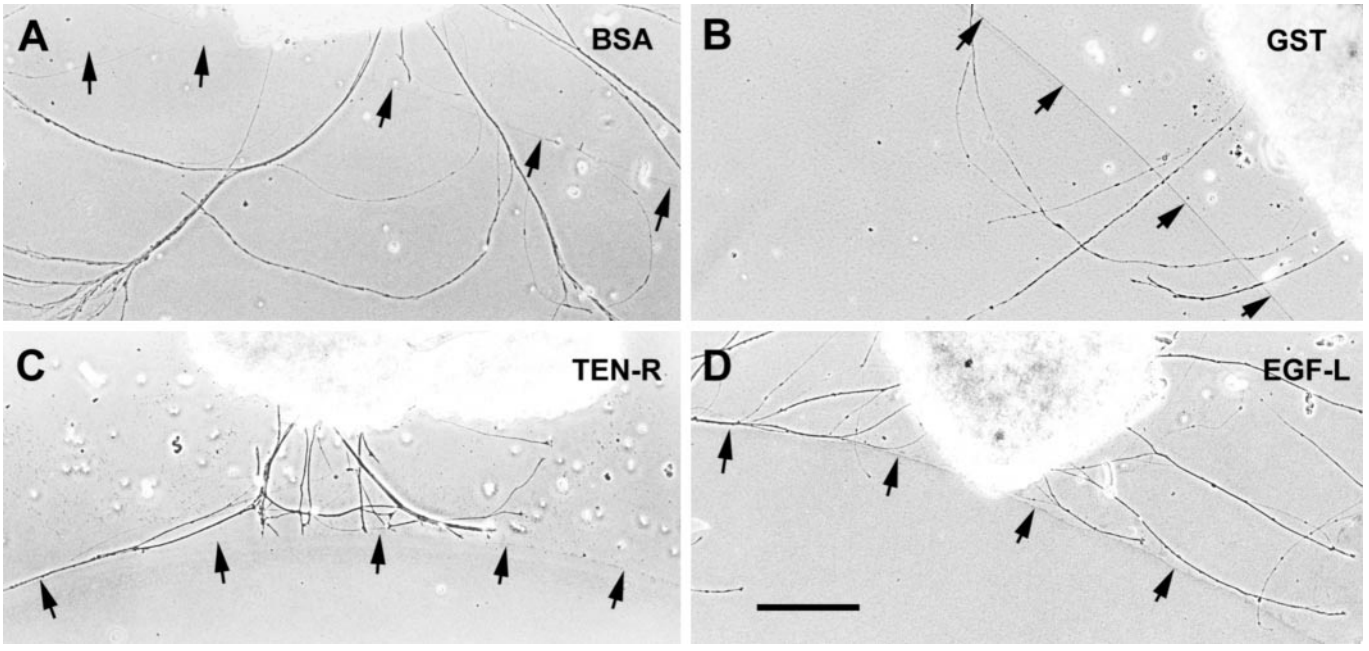

Figure 6. Behavior of retinal ganglion cell axons from retinal explants at a substrate border at 7 d *in vitro*. *A, B*, Axons mostly ignore the borders of control proteins, either BSA (*A*) or GST (*B*). *C, D*, Axons do not cross a tenascin-R (*C*) or EGF-L (*D*) border. Some axons grow along the border. There is only one thin fiber belonging to the explant shown in *D* crossing onto the test substrate. No fibers cross in *C*. *Arrows* highlight the substrate borders. Scale bar, 200 μm. *TEN-R*, Tenascin-R.

were detected in *Pleurodeles* CNS tissue makes it highly likely that the antibodies specifically recognize tenascin-R in *Pleurodeles.*

Patterns found in immunohistochemistry were also similar to those in amniotes. Immunoreactivity is only found in the CNS of amniotes and *Pleurodeles*. Prominent reactivity is found in the retinal outer plexiform layer of *Pleurodeles,* just like that in mice (Bartsch et al., 1993) and chickens (Rathjen et al., 1991). Expression was found in the adult optic nerve and at the nodes of Ranvier in CNS myelin of *Pleurodeles*, similar to mice (Bartsch et al., 1993). These similarities argue that the antibodies were specific for tenascin-R in *Pleurodeles*.

The source of tenascin-R in *Pleurodeles* appears to be both oligodendrocytes and neurons. During development and regeneration of the optic nerve, expression of tenascin-R was correlated with the appearance of myelinating oligodendrocytes, as demonstrated by MAG immunohistochemistry. Therefore, tenascin-R is likely oligodendrocyte-derived in the optic nerve of the salamander, as in mice (Bartsch et al., 1993). Expression in the unmyelinated retina and the brain before myelination takes place may be neuronal as in amniotes (Fuss et al., 1993; Wintergerst et al., 1993).

The fact that the distribution patterns of tenascin-R are similar between amphibians and amniotes suggests evolutionary conserved functions of the molecule in tetrapods. In contrast, the expression patterns of the related molecule tenascin-C are much more variable (Rettig et al., 1992; Becker et al., 1995). During development, tenascin-R may contribute to confining axonal tracts, as has been hypothesized for other inhibitory molecules (Schwab, 1990; Silver, 1994).

Tenascin-R inhibits regeneration of salamander optic fibers

Purified tenascin-R, or the bacterially expressed EGF-L fragment of tenascin-R, inhibits regeneration of adult retinal ganglion cell axons of *Pleurodeles in vitro*. Even in a mixture with laminin, which on its own strongly promotes growth of adult *Pleurodeles* retinal ganglion cell axons, tenascin-R and EGF-L inhibited neurite outgrowth from explants placed on a homogeneous substrate. Axons are not simply prevented from exiting the explants, as shown by the finding that when axons were allowed to exit the explants on a laminin substrate, they avoided growing into a region of mixed laminin–tenascin-R. Effects of tenascin-R are likely directly on the axons and not on laminin in the mixed substrates, because tenascin-R does not bind to laminin or block the neurite outgrowth-promoting properties of laminin for dorsal root ganglia in a mixed substrate (Pesheva et al., 1994). The EGF-L fragment closely mimicked the inhibitory properties of the whole molecule, indicating that inhibition of axonal growth by tenascin-R may be mediated by specific interaction with this domain. Small differences between tenascin-R and the EGF-L fragment in the two *in vitro* assays are not systematic and may simply reflect different ways of producing the two molecules. We tested amphibian optic fibers with mammalian tenascin-R *in vitro*. Although conserved apparent molecular weights, tissue distribution, and axonal reactions suggest highly similar domain structure and function of the protein in both mammals and amphibians, the definite identification of functional sites on amphibian tenascin-R has to await its molecular cloning.

Although tenascin-R is strongly inhibitory for neurite outgrowth of some cell types, it is not inhibitory for others. Retinal explants of embryonic chickens (Taylor et al., 1993), as well as embryonic and adult mice (T. Becker, B. Anlicker, C. G. Becker, J. Taylor, M. Schachner, R. L. Meyer, and U. Bartsch, unpublished observations) do not grow neurites on a homogeneous tenascin-R substrate or over a substrate border of tenascin-R. Outgrowth from cerebellar microexplants of neonatal mice is reduced and highly fasciculated on a homogeneous tenascin-R

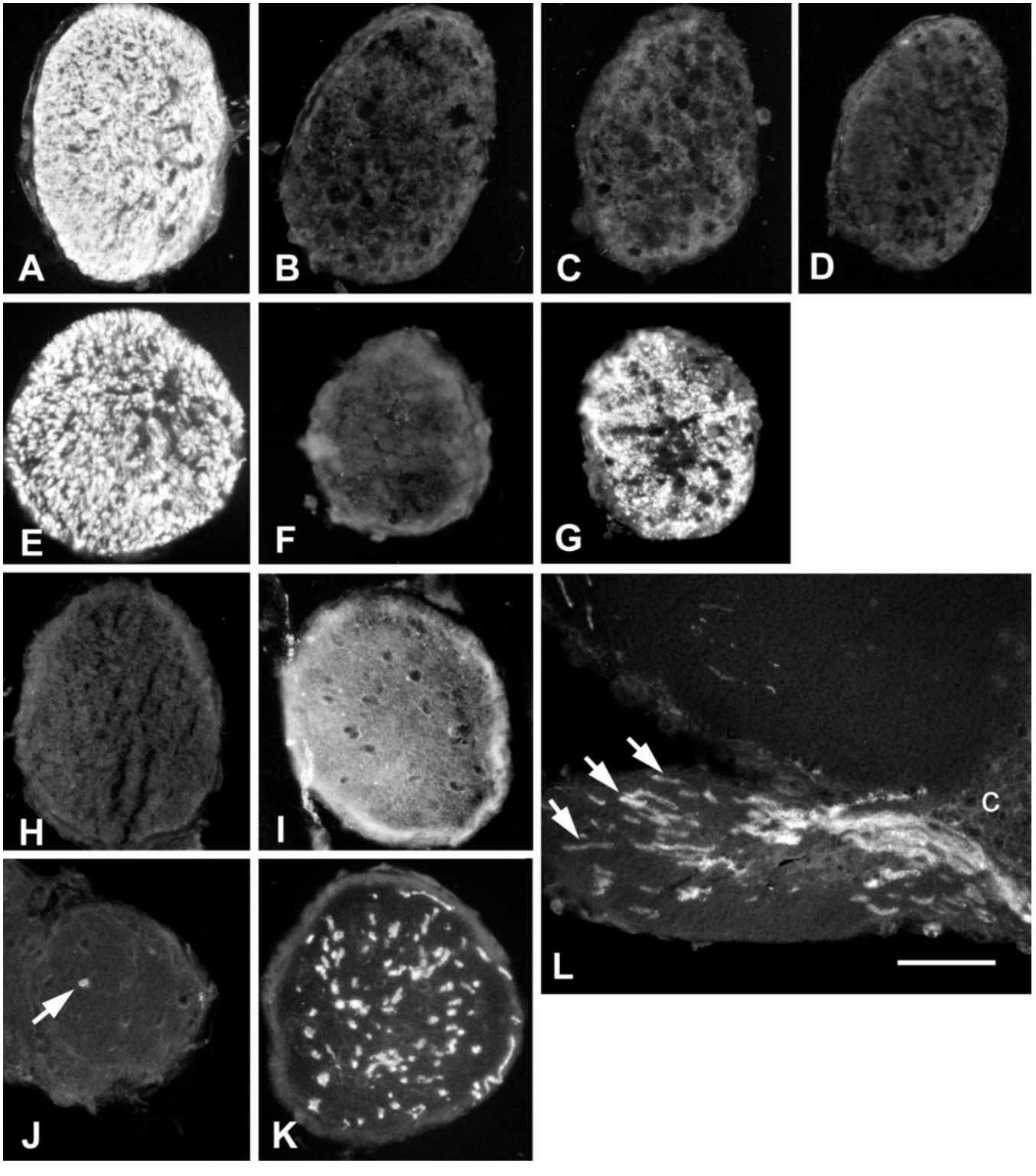

Figure 7. Comparison of tenascin-R (*A–C, H, I*) and MAG (*E–G, J–L*) immunoreactivities and control without primary antibody (*D*) in cross-sections of the crushed distal optic nerve during demyelination (*A–G*) and remyelination (*H–L*). *A,* Tenascin-R immunoreactivity is strong in unlesioned control nerves. It is reduced to undetectable levels at 8 d after the lesion in the lesion-near (*B*) and chiasm-near (*C*) parts of the distal lesioned optic nerve compared with a control without primary antibody (*D*). *E*, MAG-immunoreactive myelin sheaths are numerous in unlesioned control nerves. *F*, At 8 d after the lesion, MAG immunoreactivity is absent from the lesion-near part of the nerve. *G*, In the chiasm-near part of the nerve, MAG-immunoreactive myelin debris was present. *H, I*, Tenascin-R immunoreactivity was not detectable at 3 months after the lesion (*H*) but was detectable at 6 months after the lesion (*I*). *J*, At 3 months after the lesion, MAG immunoreactivity indicates that remyelination is scarce in the lesion-near part of the optic nerve. The *arrow* in *J* points to the only myelin sheath in this section. *L*, More myelin sheaths are present in the same animal as in *J* only in the immediate vicinity of the chiasm (*c*). *Arrows* in *L* point out some individual sheaths. Note that, for technical reasons, the nerve is cut more longitudinal at the chiasm. *K*, At 6 months after the lesion, the number of MAG-immunopositive myelin sheaths is further increased in the lesion-near part of the optic nerve. Scale bar, 75 μm.

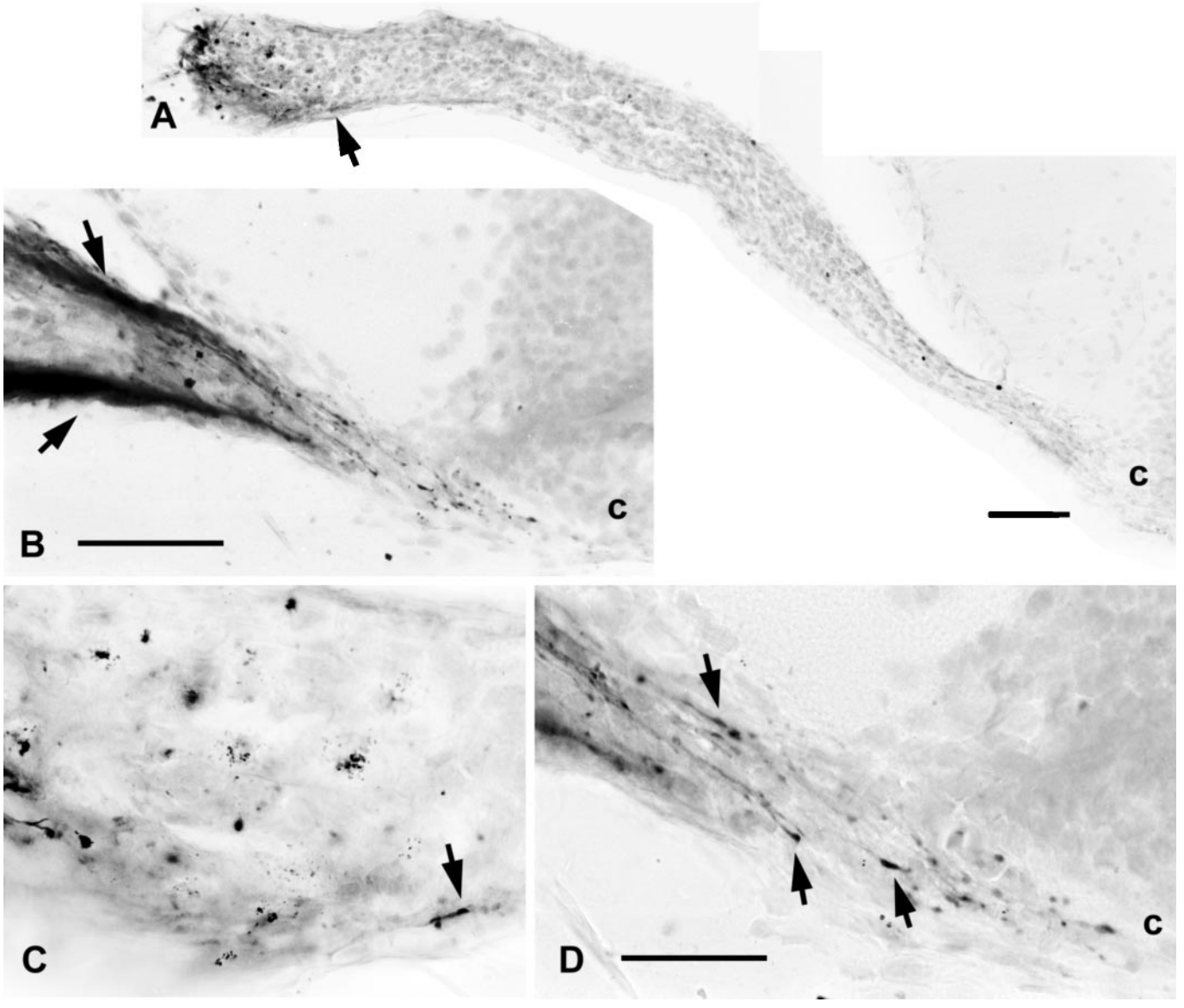

Figure 8. Anterograde labeling of regenerating axons in longitudinal sections of the distal lesioned optic nerve and chiasm at 9 (*A, C*) and 13 (*B, D*) d after the lesion at low (*A, B*) and high (*C, D*) magnification. *c*, Chiasm. *A, C*, No growth was observed at 9 d after the lesion in the distal optic nerve in this animal (The proximal nerve was cut off at the lesion site), with the exception of a single growth cone-like figure, the position of which is pointed out in *A* and *C*. This fiber is growing in the periphery of the nerve. *B, D*, At later stages of regeneration strong fascicles of axons are present in the periphery of the chiasm-near part of the nerve (*arrows* in *B*), with individual fibers tipped with growth cone-like protrusions (*arrows* in *D*) reaching the chiasm. Scale bars: *A, B*, 100 μm; *D*, 50 μm (for *C*, *D*).

substrate. Axons of chick and mouse retinal and cerebellar explants and chick dorsal root ganglia do not cross a substrate border of tenascin-R (Pesheva et al., 1993; Taylor et al., 1993).

In contrast, on a homogeneous tenascin-R substrate, outgrowth from single retinal and tectal cells of chicken (Rathjen et al., 1991; Nörenberg et al., 1995, 1996), axons of hippocampal neurons (Lochter et al., 1994, 1995; Lochter and Schachner, 1997), and also chick dorsal root ganglia is not affected or even slightly promoted, although dorsal root ganglion axons do not cross a substrate border of tenascin-R (Taylor et al., 1993). Different or opposing influences on neurite outgrowth that depend on *in vitro* assay and cell type are not unique to tenascin-R but have been shown also for other neural recognition molecules, such as tenascin-C (Lochter et al., 1991; Taylor et al., 1993), netrins (Shirasaki et al., 1996), and semaphorins (Shepherd et al., 1997). One reason for differing effects on different cell types may be that tenascin-R is a highly complex molecule with diverse functions. It may also function in neurite fasciculation (Xiao et al., 1998), oligodendrocyte differentiation (Pesheva et al., 1997), and the regulation of the microglial response to injury (Angelov et al., 1998). Therefore, the influence of tenascin-R cannot be extrapolated for all cell types and developmental stages but has to be tested for the interaction in question, as we have done here.

Removal of inhibitory molecules may facilitate axonal regeneration in amphibians

Tenascin-R immunoreactivity was no longer detectable by the time we found the first axons to regrow in the distal part of the

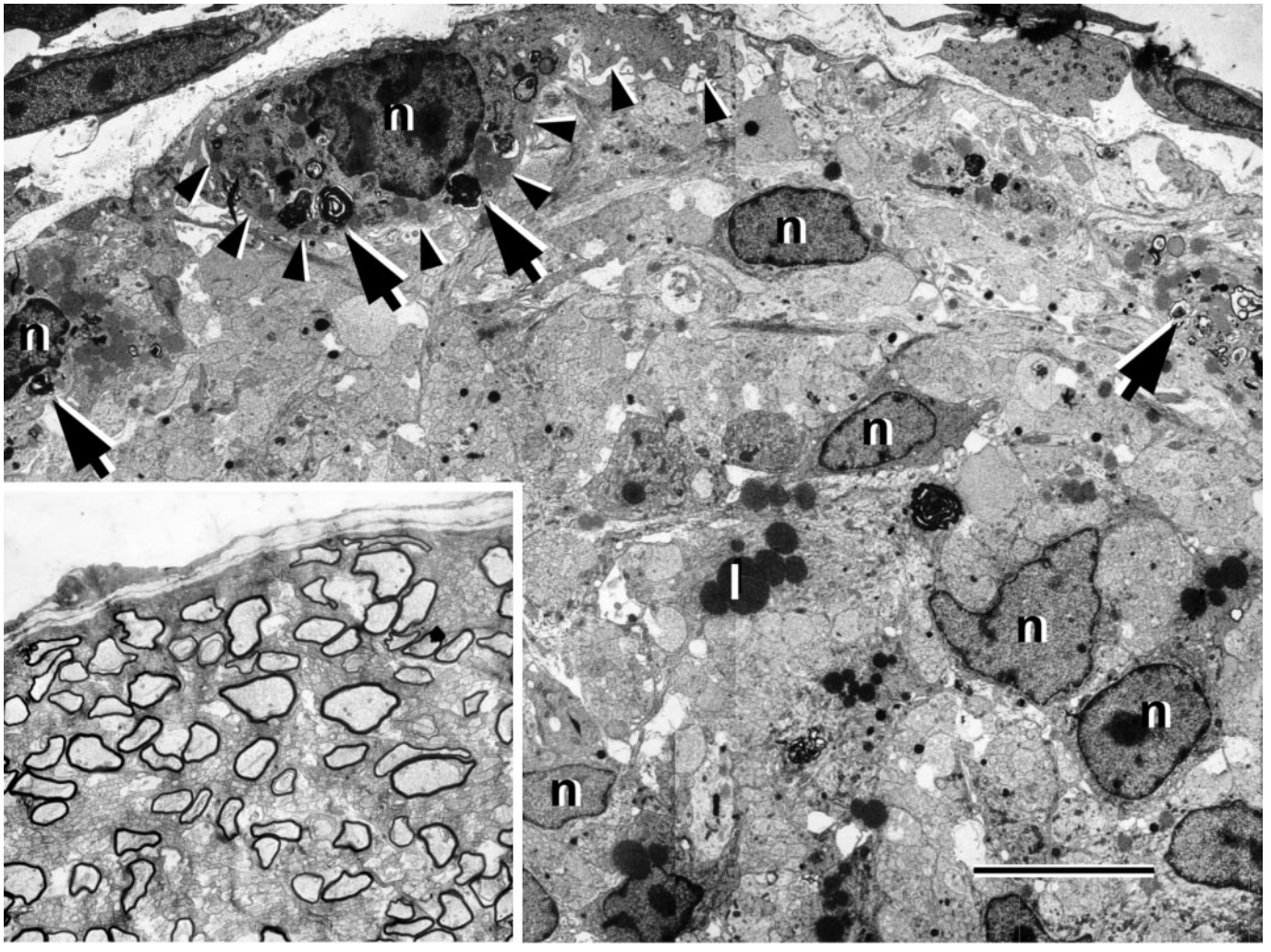

Figure 9. Electron microscopic demonstration of myelin in cross-sections of the optic nerve at 14 d after the lesion and in an unlesioned control optic nerve (*inset*). Myelin remaining in the distal optic nerve 14 d after a lesion (*arrows*) is present mostly inside the electron-dense cytoplasm of phagocytosing cells, which are often located in the periphery of the nerve. One cell is outlined with *arrowheads*. A high number of cells (*n*, nucleus) and lipid droplets (*l*) was present in the lesioned optic nerve. *Inset*, Numerous myelin sheaths are present in an unlesioned control optic nerve. Scale bar, 10 μm.

lesioned optic nerve at 9 d after the lesion. The time of onset of axonal regrowth is in agreement with other studies using electron microscopy or immunohistochemistry in salamanders (Stensaas and Feringa, 1977; Becker et al., 1993) and frogs (Bohn et al., 1982; Wilson et al., 1992). We conclude that the strong reduction of tenascin-R in the optic nerve may facilitate regrowth of retinal ganglion cell axons.

Pathway choices of regenerating axons may also contribute to the avoidance of inhibitory molecules. The close contact between protrusions of tentatively identified astrocytic radial glial processes with growing fascicles of regenerating axons we and others (Stensaas and Feringa, 1977; Wilson et al., 1992) observed in the periphery of the cross-sectioned nerve of amphibians may shield regrowing axons from residual myelin debris and inhibitory molecules, such as tenascin-R, which is likely not expressed by astrocytes. The peripheral zone of axonal regrowth is also free of the putatively inhibitory CSPGs (Smith-Thomas et al., 1995; Davies et al., 1997) found in the center of the nerve (Becker et al., 1995). Only one labeled regenerating axon was found in contact with myelin debris in the center of the chiasm-near region. Thus, contrary to the results of Turner and Singer (1974), we found that myelin debris is not a preferred substrate for axonal regrowth in the optic nerve of salamanders, similar to what has been reported for the regenerating optic nerve of goldfish (Strobel and Stuermer, 1994).

Different cell types may be involved in the removal of tenascin-R in *Pleurodeles*. We found a massive macrophage and microglial reaction after a lesion, leading to rapid phagocytosis of myelin debris, which is typical of the amphibian optic nerve (Goodbrand and Gaze, 1991; Wilson et al., 1992; Naujoks-Manteuffel and Niemann, 1994). Putative inhibitory molecules, such as MAG (McKerracher et al., 1994; Mukhopadhyay et al., 1994; Schäfer et al., 1996) (but see Bartsch et al., 1995) and tenascin-R, may be phagocytosed along with the myelin (Lang and Stuermer, 1996) by macrophages and microglial cells or radial glial cells (Goodbrand and Gaze, 1991; Phillips and Turner, 1991; Wilson et al., 1992; Naujoks-Manteuffel and Niemann, 1994). Tenascin-R could also be enzymatically degraded by proteases secreted by macrophages and microglial cells (Moore and Thanos, 1996). Oligodendrocytes, the likely source of tenascin-R in the optic nerve, could have been killed and removed along with myelin debris (Eitan and Schwartz, 1993), or they could have

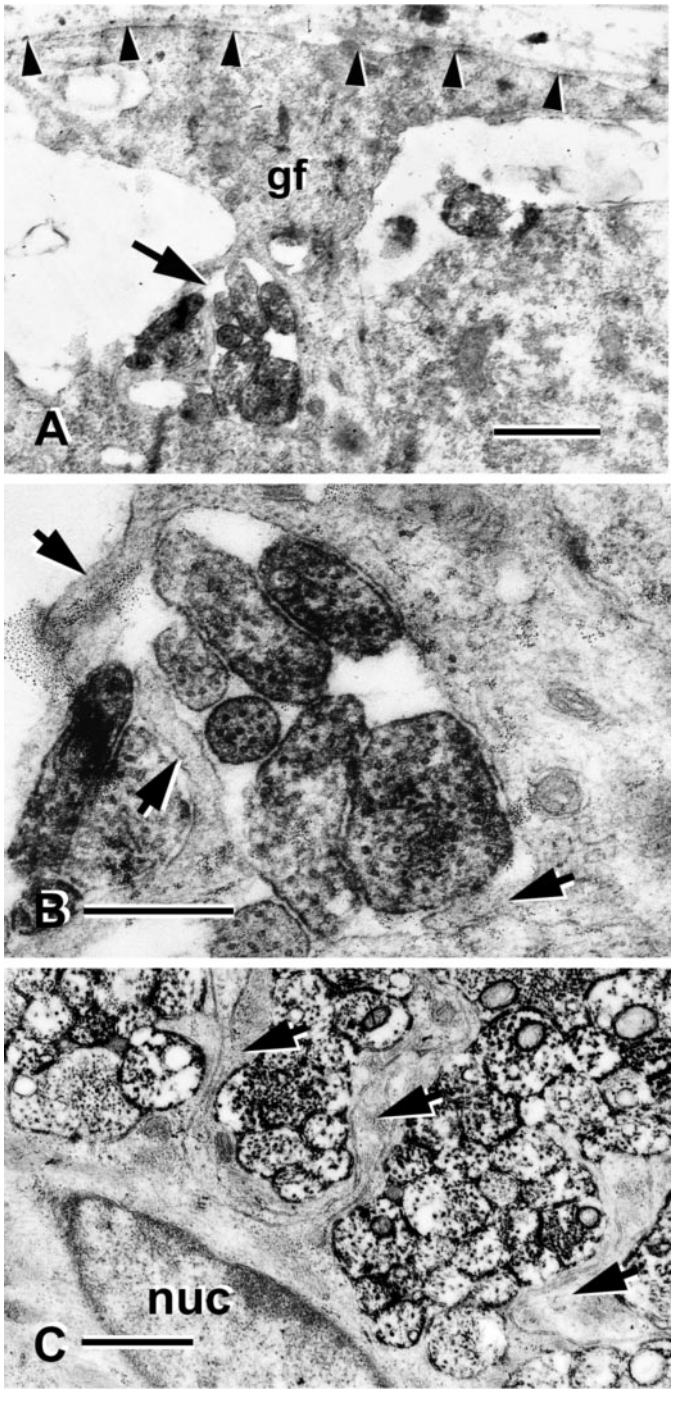

Figure 10. Electron microscopic demonstration of labeled axons in cross-sections of the optic nerve at 9 d after the lesion. *A*, A small fascicle of axons (*arrow*) in association with a presumably astrocytic glial endfoot (*gf*) was labeled in the periphery of the nerve at a distance of 300 μm from the chiasm. The contact site of the glial endfoot with the pial surface is outlined by *arrowheads*. *B*, Higher magnification of the fascicle depicted in *A*. Protrusions from the glial endfoot (*arrows*) are in close contact with the regrowing axons. *C*, In the vicinity of the lesion site at a distance of 1800 μm from the chiasm, large fascicles of axons are tightly enwrapped by processes (*arrows*) of a glial cell. *nuc*, Nucleus of the glial cell. Scale bars: *A, C*, 1 μm; *B*, 0.5 μm.

persisted but were unable to remyelinate growing axons. Remyelination recapitulates the developmental gradient beginning at the chiasm in *Pleurodeles* (Becker et al., 1995), suggesting that remyelination is accomplished by new oligodendrocytes that migrate from the diencephalic ventricular layer into the nerve.

Conclusion

Our results support the idea that regeneration of CNS tracts in salamanders is possible because molecules inhibitory to axonal regrowth are eliminated in time to allow regeneration, which may not happen in mammals. In contrast to *Pleurodeles,* in which tenascin-R is removed within days after a crush, it remains present for at least 4 weeks in mice, during which time it could inhibit axonal regrowth (Becker, Anlicker, Becker, Taylor, Schachner, Meyer, and Bartsch, unpublished observations). The slow removal of tenascin-R from the optic nerve of mice may be related to the macrophage response being much slower than in anamniotes. Consequently, myelin debris is also detectable for long times after a lesion in mammals (Perry et al., 1987; Battisti et al., 1995; Sivron and Schwartz, 1995). Elucidating the mechanisms anamniotes use to cope with inhibitory elements may provide important insights into regenerative failure in mammals.

REFERENCES

Angelov DN, Walther M, Streppel M, Guntinas-Lichius O, Neiss WF, Probstmeier R, Pesheva P (1998) Tenascin-R is antiadhesive for activated microglia that induce downregulation of the protein after peripheral nerve injury: a new role in neuronal protection. J Neurosci 18:6218–6219.

Bartsch U, Pesheva P, Raff M, Schachner M (1993) Expression of janusin (J1–160/180) in the retina and optic nerve of the developing and adult mouse. Glia 9:57–69.

Bartsch U, Bandtlow CE, Schnell L, Bartsch S, Spillmann AA, Rubin BP, Hillenbrand R, Montag D, Schwab ME, Schachner M (1995) Lack of evidence that myelin-associated glycoprotein is a major inhibitor of axonal regeneration in the CNS. Neuron 15:1375–1381.

Bastmeyer M, Beckmann M, Schwab ME, Stuermer CAO (1991) Growth of regenerating goldfish axons is inhibited by rat oligodendrocytes and CNS myelin but not by goldfish optic nerve tract oligodendrocyte-like cells and fish CNS myelin. J Neurosci 11:626–640.

Bates CA, Meyer RL (1997) The neurite-promoting effect of laminin is mediated by different mechanisms in embryonic and adult regenerating mouse optic axons in vitro. Dev Biol 181:91–101.

Battisti WP, Shinar Y, Schwartz M, Levitt P, Murray M (1992) Temporal and spatial patterns of expression of laminin, chondroitin sulphate proteoglycan and HNK-1 immunoreactivity during regeneration in the goldfish optic nerve. J Neurocytol 21:557–573.

Battisti WP, Wang J, Bozek K, Murray M (1995) Macrophages, microglia, and astrocytes are rapidly activated after crush injury of the goldfish optic nerve: a light and electron microscopic analysis. J Comp Neurol 354:306–320.

Becker CG, Becker T, Schachner M (1996) Tenascin-R (Janusin) is not expressed during axon regrowth in the lesioned salamander optic nerve. In: Brain and evolution (Schnitzler HU, Elsner N, eds), p 435. Stuttgart: Thieme.

Becker T, Becker CG, Niemann U, Naujoks-Manteuffel C, Gerardy-Schahn R, Roth G (1993) Amphibian-specific regulation of polysialic acid and the neural cell adhesion molecule in development and regeneration of the retinotectal system of the salamander *Pleurodeles waltl*. J Comp Neurol 336:532–544.

Becker T, Becker CG, Niemann U, Naujoks-Manteuffel C, Bartsch U, Schachner M, Roth G (1995) Immunohistological localization of tenascin-C in the developing and regenerating retinotectal system of two amphibian species. J Comp Neurol 360:643–657.

Becker T, Becker CG, Meyer RL, Schachner M (1997a) Tenascin-R is present in the CNS of anamniotes and inhibits axonal outgrowth. Soc Neurosci Abstr 676.18.

Becker T, Wullimann MF, Becker CG, Bernhardt RR, Schachner M (1997b) Axonal regrowth after spinal cord transection in adult zebrafish. J Comp Neurol 377:577–595.

Bohn RC, Reier PJ, Sourbeer EB (1982) Axonal interactions with connective tissue and glial substrata during optic nerve regeneration in *Xenopus* larvae and adults. Am J Anat 165:397–419.

Caroni P, Schwab ME (1988) Antibody against myelin-associated inhibitor of neurite growth neutralizes nonpermissive properties of CNS white matter. Neuron 1:85–96.

Davies SJA, Fitch MT, Memberg SP, Hall AK, Raisman G, Silver J (1997) Regeneration of adult axons in white matter tracts of the central nervous system. Nature 390:680–683.

Eitan S, Schwartz M (1993) A transglutaminase that converts interleukin-2 into a factor cytotoxic to oligodendrocytes. Science 261:106–108.

Faissner A, Steindler D (1995) Boundaries and inhibitory molecules in developing neural tissues. Glia 13:233–254.

Fuss B, Wintergerst ES, Bartsch U, Schachner M (1993) Molecular characterization and in situ messenger RNA localization of the neural recognition molecule J1–160/180—a modular structure similar to tenascin. J Cell Biol 120:1237–1249.

Gallien L, Durocher M (1957) Table chronologique du developpement chez *Pleurodeles waltlii michah*. Bull Biol Fr Belg 91:97–114.

Gaze RM (1970) The formation of nerve connections. London: Academic.

Goodbrand IA, Gaze RM (1991) Microglia in tadpoles of *Xenopus laevis*: normal distribution and the response to optic nerve injury. Anat Embryol 184:71–82.

Grant P, Tseng Y (1986) Embryonic and regenerating *Xenopus* retinal fibers are intrinsically different. Dev Biol 114:475–491.

Lagenaur C, Lemmon V (1987) An L1-like molecule, the 8D9 antigen, is a potent substrate for neurite extension. Proc Natl Acd Sci USA 84:7753–7757.

Lang DM, Stuermer CAO (1996) Adaptive plasticity of *Xenopus* glial cells in vitro and after CNS fiber tract lesions in vivo. Glia 18:92–106.

Lang DM, Rubin BP, Schwab ME, Stuermer CAO (1995) CNS myelin and oligodendrocytes of the *Xenopus* spinal cord—but not optic nerve—are nonpermissive for axon growth. J Neurosci 15:99–109.

Lochter A, Schachner M (1997) Inhibitors of protein kinases abolish ECM-mediated promotion of neuronal polarity. Exp Cell Res 235:124–129.

Lochter A, Vaughan L, Kaplony A, Prochiantz A, Schachner M, Faissner A (1991) J1/Tenascin in substrate-bound and soluble form displays contrary effects on neurite outgrowth. J Cell Biol 113:1159–1171.

Lochter A, Taylor J, Fuss B, Schachner M (1994) The extracellular matrix molecule janusin regulates neuronal morphology in a substrate- and culture time-dependent manner. Eur J Neurosci 6:597–606.

Lochter A, Taylor J, Braunewell KH, Holm J, Schachner M (1995) Control of neuronal morphology in vitro: interplay between adhesive substrate forces and molecular instruction. J Neurosci Res 42:145–158.

Martin GF, Ghooray GT, Wang XM, Xu XM, Zou XC (1994) Models of spinal cord regeneration. In: Neural regeneration (Seil FJ, ed), pp 175–201. Amsterdam: Elsevier.

McKerracher L, David S, Jackson DL, Kottis V, Dunn RJ, Braun PE (1994) Identification of myelin-associated glycoprotein as a major myelin-derived inhibitor of neurite growth. Neuron 13:805–811.

McQuarrie IG, Grafstein B (1981) Effect of a conditioning lesion on optic nerve regeneration in goldfish. Brain Res 216:253–264.

Meyer RL, Miotke J (1990) Rapid initiation of neurite outgrowth onto laminin from explants of adult mouse retina induced by optic nerve crush. Exp Neurol 107:214–221.

Moore S, Thanos S (1996) The concept of microglia in relation to central nervous system disease and regeneration. Prog Neurobiol 48:441–445.

Mukhopadhyay G, Doherty P, Walsh FS, Crocker PR, Filbin MT (1994) A novel role for myelin-associated glycoprotein as an inhibitor of axonal regeneration. Neuron 13:757–767.

Naujoks-Manteuffel C, Niemann U (1994) Microglial cells in the brain of *Pleurodeles waltl* (Urodela, Salamandridae) after Wallerian degeneration in the primary visual system using *Bandeiraea simplicifolia* isolectin B-4-cytochemistry. Glia 10:101–113.

Nörenberg U, Hubert M, Brümmendorf T, Tárnok A, Rathjen FG (1995) Characterization of functional domains of the tenascin-R (restrictin) polypeptide: cell attachment site, binding with F11, and enhancement of F11-mediated neurite outgrowth by tenascin-R. J Cell Biol 130:473–484.

Nörenberg U, Hubert M, Rathjen FG (1996) Structural and functional characterization of tenascin-R (restrictin), an extracellular matrix glycoprotein of glial cells and neurons. Int J Dev Neurosci 14:217–231.

Perry VH, Brown MC, Gordon S (1987) The macrophage response to central and peripheral nerve injury. J Exp Med 165:1218–1223.

Pesheva P, Spiess E, Schachner M (1989) J1–160 and J1–180 are oligodendrocyte-secreted nonpermissive substrates for cell adhesion. J Cell Biol 109:1765–1778.

Pesheva P, Gennarini G, Goridis C, Schachner M (1993) The F3/11 cell adhesion molecule mediates the repulsion of neurons by the extracellular matrix glycoprotein J1–160/180. Neuron 10:69–82.

Pesheva P, Probstmeier R, Skubitz APN, McCarthy JB, Furcht LT, and Schachner M (1994) Tenascin-R (J1 160; 180) inhibits fibronectin-mediated cell adhesion—functional relatedness to tenascin-C. J Cell Sci 107:2323–2333.

Pesheva P, Gloor S, Schachner M, Probstmeier R (1997) Tenascin-R is an intrinsic autocrine factor for oligodendrocyte differentiation and promotes cell adhesion by a sulfatide-mediated mechanism. J Neurosci 17:4642–4651.

Phillips LL, Turner JE (1991) Biphasic cellular response to transection in the newt optic nerve—glial reactivity precedes axonal degeneration. J Neurocytol 20:51–64.

Rathjen FG, Wolff JM, Chiquet-Ehrismann R (1991) Restrictin—a chick neural extracellular matrix protein involved in cell attachment co-purifies with the cell recognition molecule F11. Development 113:151–164.

Rettig WJ, Hoffman S, Su SL, Garinchesa P (1992) Species diversity of neuronectin and cytotactin expression patterns in the vertebrate central nervous system. Brain Res 590:219–228.

Schäfer M, Fruttiger M, Montag D, Schachner M, Martini R (1996) Disruption of the gene for the myelin associated glycoprotein improves axonal regrowth along myelin in C57BL/wld(S) mice. Neuron 16:1107–1113.

Schwab ME (1990) Myelin-associated inhibitors of neurite growth. Exp Neurol 109:2–5.

Shepherd IT, Luo YL, Lefcort F, Reichardt LF, Raper JA (1997) A sensory axon repellent secreted from ventral spinal cord explants is neutralized by antibodies raised against collapsin-1. Development 124:1377–1385.

Shirasaki R, Mirzayan C, Tessier-Lavigne M, Murakami F (1996) Guidance of circumferentially growing axons by netrin-dependent and -independent floor plate chemotropism in the vertebrate brain. Neuron 17:1079–1088.

Silver J (1994) Inhibitory molecules in development and regeneration. J Neurol 242:S22–S24.

Sivron T, Schwartz M (1994) The enigma of myelin-associated growth inhibitors in spontaneously regenerating nervous systems. Trends Neurosci 17:277–281.

Sivron T, Schwartz M (1995) Glial cell types, lineages, and response to injury in rat and fish: implications for regeneration. Glia 13:157–165.

Sivron T, Schwab ME, Schwartz M (1994) Presence of growth inhibitors in fish optic nerve myelin—postinjury changes. J Comp Neurol 343:237–246.

Smith-Thomas LC, Fokseang J, Stevens J, Du JS, Muir E, Faissner A, Geller HM, Rogers JH, Fawcett JW (1994) An inhibitor of neurite outgrowth produced by astrocytes. J Cell Sci 107:1687–1695.

Smith-Thomas LC, Stevens J, Fokseang J, Faissner A, Rogers JH, Fawcett JW (1995) Increased axon regeneration in astrocytes grown in the presence of proteoglycan synthesis inhibitors. J Cell Sci 108:1307–1315.

Steindler DA, Cooper NGF, Faissner A, Schachner M (1989) Boundaries defined by adhesion molecules during development of the cerebral cortex: the J1/tenascin glycoprotein in the mouse somatosensory cortical barrel field. Dev Biol 131:243–260.

Stensaas LJ, Feringa ER (1977) Axon regeneration across the site of injury in the optic nerve of the newt *Triturus pyrrhogaster*. Cell Tissue Res 179:501–516.

Strobel G, Stuermer CAO (1994) Growth cones of regenerating retinal axons contact a variety of cellular profiles in the transected goldfish optic nerve. J Comp Neurol 346:435–448.

Taylor JSH, Jack JL, Easter Jr SS (1989) Is the capacity for optic nerve

regeneration related to continued retinal ganglion cell production in the frog? A test of the hypothesis that neurogenesis and axon regeneration are obligatory linked. Eur J Neurosci 1:626–638.

Taylor J, Pesheva P, Schachner M (1993) Influence of janusin and tenascin on growth cone behavior in vitro. J Neurosci Res 35:347–362.

Turner JE, Singer M (1974) The ultrastructure of regeneration in the severed newt optic nerve. J Exp Zool 190:249–268.

Wanner M, Lang DM, Bandtlow CE, Schwab ME, Bastmeyer M, Stuermer CAO (1995) Reevaluation of the growth-permissive substrate properties of goldfish optic nerve myelin and myelin proteins. J Neurosci 15:7500–7508.

Wilson MA, Gaze RM, Goodbrand IA, Taylor JSH (1992) Regeneration in the *Xenopus* tadpole optic nerve is preceded by a massive macrophage/microglial response. Anat Embryol 186:75–89.

Wintergerst ES, Fuss B, Bartsch U (1993) Localization of janusin messenger RNA in the central nervous system of the developing and adult mouse. Eur J Neurosci 5:299–310.

Xiao ZC, Taylor J, Montag D, Rougon G, Schachner M (1996) Distinct effects of recombinant tenascin-R domains in neuronal cell functions and identification of the domain interacting with the neuronal recognition molecule F3/11. Eur J Neurosci 8:766–782.

Xiao ZC, Revest JM, Laeng P, Rougon G, Schachner M, Montag D (1998) Defasciculation of neurites is mediated by tenascin-R and its neuronal receptor F3/11. J Neurosci Res 52:390–404.